Determination of weak anisotropy parameters from the qP wave slowness and particle motion measurements in laterally homogeneous media [1]

Xuyao Zheng and **Ivan Pšenčík**

Geophysical Institute, Acad.Sci.of Czech Republic, Boční II, Praha 4, Czech Republic;
e-mail: zheng@ig.cas.cz, ip@ig.cas.cz

ABSTRACT

Results of synthetic tests of the procedure for local evaluation of weak anisotropy (WA) parameters at receivers in a borehole in a multi- azimuthal multiple-source offset VSP experiment are presented. The WA parameters are determined from measurements of slowness vectors and/or deviations of measured qP wave particle motions from the corresponding slowness vectors at individual receivers. Considered medium is assumed to be weakly anisotropic with anisotropy of arbitrary symmetry. Certain limitation of the presented procedure is requirement of lateral homogenity of the medium. Basic formulae and synthetic examples of their application are presented.

INTRODUCTION

We present results of synthetics tests of the modified procedure proposed by Pšenčík and Zheng (1998). The procedure represents a generalization of the procedures proposed by Gaiser (1990) or Horne et al. (1998). In presented procedure, local parameters of a medium are determined by inverting data obtained during a multi-azimuthal multiple-source offset VSP experiment with three-component recordings not affected by a free surface. Studied medium is assumed to be vertically inhomogeneous and weakly anisotropic with anisotropy of arbitrary symmetry. For this medium, we find a background isotropic medium, from which the weakly anisotropic medium differs only slightly. Then we can express the qP wave slowness and the polarization vector in the weakly anosotropic medium using the formulae relating them linearly to the so-called weak anisotropy (WA) parameters specifying anisotropy of the medium. If the qP wave slowness and polarization vector are known, the formulae can be understood as a system of linear algebraic equations for determination of the WA parameters. The determination of the polarization vector from observations is straightforward. The determination of the slowness vector (from which slowness can be determined) is more complicated. We use a generalization of the approach proposed by

[1] Seismic Waves in Complex 3-D Structures, Report 8 (Department of Geophysics, Charles University, Prague 1998), pp.47-62

Gaiser (1990). The vertical component of the slowness vector of the studied wave is determined from its travel times recorded in the borehole. As Gaiser (1990), we assume that the medium is laterally homogeneous. This assumption allows us to make use of travel time reciprocity and to determine the horizontal inline and crossline components of the slowness vector from travel times between sources and a given receiver. Note that instead of a VTI medium considered by Gaiser(1990) we consider a weakly anisotropic medium of arbitrary symmetry. Thus, in contrast to Gaiser's laterally homogeneous VTI medium, in which the slowness vector always remains confined to the vertical plane containing the source and the borehole, the slowness vector in our model can deviate from that plane. When the slowness vector and the polarization vector are known, an overdetermined system of linear equations for WA parameters at each receiver can be constructed.

BASIC FORMULAE

We consider a right-handed Cartesian coordinate system with $x-$ and $y-$axes horizontal and $z-$axis vertical, positive downwards. We can express P wave slowness c^{-1} and the polarization vector g_i in the WA medium using the formulae derived by Pšenčík and Zheng (1998), see also Pšenčík and Gajewski (1998)

$$c^{-1} \sim \alpha^{-1}(1-\frac{B_{33}}{2\alpha^2}), \tag{1}$$

$$g_i \sim n_i + \alpha p_k e_k^{(1)} e_i^{(1)} + \alpha p_k e_k^{(2)} e_i^{(2)} + \frac{B_{13} e_i^{(1)}}{\alpha^2-\beta^2} + \frac{B_{23} e_i^{(2)}}{\alpha^2-\beta^2}. \tag{2}$$

The symbol p_i denotes the slowness vector in the WA medium, $p_k p_k = c^{-2}$. The vectors $e_i^{(1)}$, $e_i^{(2)}$ and $n_i = e_i^{(3)}$ are three mutually perpendicular unit vectors defined at a receiver on a ray of a P wave in the background isotropic medium. The isotropic medium is characterized by the P and S wave velocities α and β. The vector n_i is tangent to the ray, the vectors $e_i^{(1)}$ and $e_i^{(2)}$ can be chosen arbitrarily in the plane perpendicular to n_i. We choose them so that all three vectors read

$$\vec{e}^{(1)} = D^{-1}(n_1n_3, n_2n_3, n_3^2-1), \quad \vec{e}^{(2)} = D^{-1}(-n_2, n_1, 0), \quad \vec{e}^{(3)} = \vec{n} = (n_1, n_2, n_3), \tag{3}$$

where

$$D = (n_1^2+n_2^2)^{1/2}, \quad n_1^2+n_2^2+n_3^2 = 1. \tag{4}$$

The symbols B_{mn} in Eqs.(1) and (2) denote elements of the weak anisotropy matrix, see Pšenčík & Gajewski (1998). The explicit expressions for B_{33}, B_{13} and B_{23} read:

$$\begin{aligned} B_{33} = 2\alpha^2[&\epsilon_z n_3^4 + 2n_3^3(\epsilon_{34}n_2+\epsilon_{35}n_1) + n_3^2(\delta_x n_1^2 + \delta_y n_2^2 + 2\chi_z n_1 n_2) \\ &+2n_3(\chi_x n_1^2 n_2 + \chi_y n_1 n_2^2 + \epsilon_{15} n_1^3 + \epsilon_{24} n_2^3) \\ &+\epsilon_x n_1^4 + \delta_z n_1^2 n_2^2 + \epsilon_y n_2^4 + 2\epsilon_{16} n_1^3 n_2 + 2\epsilon_{26} n_1 n_2^3], \end{aligned} \tag{5}$$

$$B_{13} = \alpha^2 D^{-1}\{2\epsilon_z n_3^5 + n_3^4(\epsilon_{34}n_2+\epsilon_{35}n_1) + n_3^3(\delta_x n_1^2 + \delta_y n_2^2 + 2\chi_z n_1 n_2 - 2\epsilon_z)$$

$$+n_3^2[(4\chi_x - 3\epsilon_{34})n_1^2n_2 + (4\chi_y - 3\epsilon_{35})n_1n_2^2 + (4\epsilon_{15} - 3\epsilon_{35})n_1^3 + (4\epsilon_{24} - 3\epsilon_{34})n_2^3]$$
$$+n_3[(2\delta_z - \delta_x - \delta_y)n_1^2n_2^2 + 2(2\epsilon_{16} - \chi_z)n_1^3n_2 + 2(2\epsilon_{26} - \chi_z)n_1n_2^3$$
$$+(2\epsilon_x - \delta_x)n_1^4 + (2\epsilon_y - \delta_y)n_2^4] - \chi_xn_1^2n_2 - \chi_yn_1n_2^2 - \epsilon_{15}n_1^3 - \epsilon_{24}n_2^3\}, \qquad (6)$$
$$B_{23} = \alpha^2D^{-1}\{n_3^3(\epsilon_{34}n_1 - \epsilon_{35}n_2) + n_3^2[(\delta_y - \delta_x)n_1n_2 + \chi_zn_1^2 - \chi_zn_2^2]$$
$$+n_3[(2\chi_y - 3\epsilon_{15})n_1^2n_2 - (2\chi_x - 3\epsilon_{24})n_1n_2^2 + \chi_xn_1^3 - \chi_yn_2^3]$$
$$+(\delta_z - 2\epsilon_x)n_1^3n_2 + (2\epsilon_y - \delta_z)n_1n_2^3 + 3(\epsilon_{26} - \epsilon_{16})n_1^2n_2^2 + \epsilon_{16}n_1^4 - \epsilon_{26}n_2^4\}. \qquad (7)$$

The coefficients of the directional cosines n_i in Eqs.(5), (6) and (7) are the qP wave weak anisotropy parameters. They are defined as follows

$$\epsilon_x = \frac{A_{11} - \alpha^2}{2\alpha^2}, \quad \epsilon_y = \frac{A_{22} - \alpha^2}{2\alpha^2}, \quad \epsilon_z = \frac{A_{33} - \alpha^2}{2\alpha^2},$$
$$\delta_x = \frac{A_{13} + 2A_{55} - \alpha^2}{\alpha^2}, \quad \delta_y = \frac{A_{23} + 2A_{44} - \alpha^2}{\alpha^2}, \quad \delta_z = \frac{A_{12} + 2A_{66} - \alpha^2}{\alpha^2},$$
$$\chi_x = \frac{A_{14} + 2A_{56}}{\alpha^2}, \quad \chi_y = \frac{A_{25} + 2A_{46}}{\alpha^2}, \quad \chi_z = \frac{A_{36} + 2A_{45}}{\alpha^2},$$
$$\epsilon_{15} = \frac{A_{15}}{\alpha^2}, \quad \epsilon_{16} = \frac{A_{16}}{\alpha^2}, \quad \epsilon_{24} = \frac{A_{24}}{\alpha^2}, \quad \epsilon_{26} = \frac{A_{26}}{\alpha^2}, \quad \epsilon_{34} = \frac{A_{34}}{\alpha^2}, \quad \epsilon_{35} = \frac{A_{35}}{\alpha^2}. \qquad (8)$$

We can see that the qP wave slowness and the polarization vector are fully controlled by 15 WA parameters. We rewrite now Eqs.(1) and (2) into the form, in which the unknown WA parameters appear on the LHS of equations through the terms B_{mn} and equations are in the form convenient for solving. Rewritten equations read

$$B_{33} = 2\alpha^2(1 - \alpha c^{-1}), \qquad (9)$$

and

$$B_{13} = (\alpha^2 - \beta^2)(g_ke_k^{(1)} - \alpha p_ke_k^{(1)}), \quad B_{23} = (\alpha^2 - \beta^2)(g_ke_k^{(2)} - \alpha p_ke_k^{(2)}). \qquad (10)$$

Equations (9) and (10) represent a system of linear algebraic equations for 15 unknown WA parameters. As described above, the polarization vector g_i as well as the slowness vector p_i can be determined from observations. With the slowness vector and polarization vector known, we have $3N_SN_A$ equations for 15 WA parameters at each receiver. Here N_S denotes the number of sources along a profile and N_A the number of profiles. At least 5 profiles are necessary for the determination of all qP wave WA parameters from the slowness formula (1), see Pšenčík and Gajewski (1998). Only 3 profiles are sufficient for the determination of the WA parameters from the formula for the polarization vector, see Eqs.(6) and (7). Thus combination of both formulae can lead to a reduction of measurement requirements.

INVERSION OF SYNTHETIC DATA

Considered model and configuration of the synthetic experiment is the same as that of Liu and Pšenčík (1999). The model box is specified as follows: x is in the interval $< -1.0, 1.0 >$, y in $< -1.0, 1.0 >$ and z in $< 0.0, 0.7 >$ km. The medium in the model box is vertically inhomogeneous, hexagonally symmetric, and it is specified by the following matrix of density normalized elastic parameters (in km^2/s^2)

$$\begin{pmatrix} 15.71 & 5.05 & 4.46 & 0.00 & 0.00 & 0.00 \\ & 15.71 & 4.46 & 0.00 & 0.00 & 0.00 \\ & & 13.39 & 0.00 & 0.00 & 0.00 \\ & & & 4.98 & 0.00 & 0.00 \\ & & & & 4.98 & 0.00 \\ & & & & & 5.33 \end{pmatrix} .$$

at the $z = 0.0$ km and by

$$\begin{pmatrix} 19.64 & 6.31 & 5.58 & 0.00 & 0.00 & 0.00 \\ & 19.64 & 5.58 & 0.00 & 0.00 & 0.00 \\ & & 16.74 & 0.00 & 0.00 & 0.00 \\ & & & 6.23 & 0.00 & 0.00 \\ & & & & 6.23 & 0.00 \\ & & & & & 6.66 \end{pmatrix} .$$

at $z = 1.0$ km. The axis of symmetry (specified as vertical in the above matrices) is rotated by 80^o from vertical around the y-axis and by 25^o from the x-axis in the considered model.

We consider a synthetic multi-azimuthal multiple-source offset VSP experiment. The borehole is situated in the coordinate origin. There are 13 receivers distributed evenly within the borehole, They are distributed with the step of 0.05 km starting at the depth of 0.1 km. The effects of the free surface are neglected. Six profiles, 0^o, 30^o, 60^o, 90^o, 120^o and 150^o (measured counterclockwise from the x-axis) intersecting at the mouth of the borehole are considered. There are 9 evenly distributed sources on each profile on each side of the borehole, see the bottom part of Figure 1. The closest source is situated 0.1 km from the borehole, the step between the sources is also 0.1 km. In this way, we have 108 observations at each receiver at our disposal. In the upper part of Figure 1 straight lines connecting sources and receivers (and simulating rays) situated in the (x, z) plane are shown. We can see that the "ray" angular coverage at the top of the model is rather good. The shallowest receiver is illuminated both by nearly horizontal "rays" (from the most distant sources) and by nearly vertical "rays" (from the sources closest to the borehole). The situation at the deepest receivers is not so good. The deepest receivers are illuminated well by nearly vertical "rays" but there are no horizontal and nearly horizontal "rays" illuminating these receivers. We must therefore expect worse results of inversion for the deeper part of the model. The "observed" synthetics for the described configuration were calculated by a modified version of the ANRAY program package, see Gajewski and Pšenčík (1990).

Arrival times and polarization directions were determined from "observed" synthetic seismograms. At each receiver the arrival times were first used for the determination of a background P wave velocity α (S wave velocity β was taken as $\alpha/\sqrt{3}$), second for the determination of vertical and horizontal inline components of the slowness vector. Since the crossline component resulting from the measurements was substantially smaller than the vertical and inline components, we made a simplified assumption about the slowness vector that its crossline component is zero. The background isotropic model was determined as vertically inhomogeneous. Rays were traced in this model from the sources on surface profiles to the receivers in the borehole. The vectors $e_i^{(1)}$, $e_i^{(2)}$ and n_i were then determined on these rays at receivers according to Eqs.(3). In this way, all the necessary coefficients of Eqs.(9) and (10) were determined. Since the system of Eqs.(9) and (10) is linear, we solved it iteratively by a gradient method.

The results based on the data recorded from all 6 profiles are shown in Fig.2. Three blocks, from the top to the bottom, show results using "slowness" formula only, i.e. Eq.(9) (top), "polarization" formula only, i.e. Eq.(10) (middle) and both "slowness" and "polarization" formulae (bottom). In each block, results for three selected receivers situated at depths $z = 0.25$, 0.45 and 0.65 km are shown. For each depth, projections of the exact axis of symmetry (full line) and the axis of symmetry found by solving Eq.(9) and/or (10) (dashed line) into (x, z), (x, y) and (y, z) planes are shown. The rightest plots show sections of phase velocity surfaces by planes containing the axis of symmetry. The horizontal axis shows angles (in degrees) measured from the axis of symmetry (0^o) to the plane of isotropy (90^o), the vertical axis shows the phase velocity. We can see a nearly perfect fit of inverted and true data. It seems that the combined use of the slowness and polarization yields slightly better results than the use of the slowness and polarization separately. As expected, slightly worse results are obtained for the deepest receiver. This is a consequence of insufficient illumination of the deeper receivers discussed above.

In Figure 3, effects of a reduced number of profiles with sources on the quality of the inversion can be studied. Instead of the complete set of 6 profiles, only 3 profiles are considered: 0^o, 60^o, and 120^o. As mentioned above, this is less number of profiles than necessary for a complete recovery of the WA parameters from the "slowness" formula and just a minimum required for a complete recovery of the WA parameters from the "polarization" formula. We can see that the results are now slightly worse, especially orientation of the determined symmetry axis in the (x, y) plane and in the form of the angular phase velocity variation. Nevertheless, basic features of the true model are preserved. Surprisingly, the "slowness" formula yields results of comparable quality with the "slowness" formula. Combination of both formulae yields slightly better results again.

Following figures show influence of the noise in data on the inversion. Figure 4 shows the same results as Figure 2 but the "observed" data contain 10% noise. Except slight discrepancies between the orientation of the inverted and true symmetry axis in the (x, y) plane, there are no remarkable differences from Figure 2. Figure 5 shows the results for the same level of noise but for data obtained from 3 profiles only, as in Figure 3. Here the effects in the (x, y) plane are stronger. In some phase velocity sections, however, the fit between inverted and true phase velocities seems to be even better than in Figure 3.

The 20% noise has the same negligible effects on inversion of data from all 6 profiles, see Figure 6. Some effects of this level of noise seem to appear in Figure 7 showing the results of inversion of data from 3 profiles, in the results obtained from "slowness" formula. Substantial effects can be observed in results obtained from data with 30% noise shown in Figures 8 (inversion of data from 6 profiles) and 9 (inversion of data from 3 profiles). The "slowness" formula seems to yield slightly better results than "polarization" formula. The "polarization" formula probably affects the results of the combination of both formulae so that they are worse than results of the "slowness" formula alone. Results of the "slowness" formula for data from 6 profiles still have acceptable quality. Results of the "polarization" formula or of the combination of both formulae are significantly distorted. Further increase of the noise level would lead to even more severe distortions.

Except the inversion of data with 30% noise, the use of combination of the "slowness" and "polarization" formulae seems to lead to better results.

CONCLUSIONS

First tests with synthetic data indicate that the proposed inversion scheme could be used for the local determination of WA parameters at receivers situated in weakly anisotropic media of arbitrary symmetry even under simplifying assumptions of inline oriented slowness vector. Tests with reduced number of profiles seem to indicate that a combination of the "slowness" and "polarization" formulae leads to better results. Tests with noisy data indicate that the "slowness" formula is a more reliable tool for the determination of the WA parameters.

Of course, further tests are necessary to confirm the above conclusions. We plan to perform tests with irregular distribution of source profiles and reduced number of sources. Tests of effects of lateral variation of the structure and of lower symmetry anisotropy are also desirable. We plan to concentrate on media, which cause a significant deviation of the slowness vector from the propagation plane. It would be also very useful to test the proposed procedure on data from a real experiment.

In addition to the above tests, certain generalizations of the proposed procedure can be also made. It would not be difficult to generalize the procedure for a less ideal case of non-vertical borehole, receiver twist, different source elevations, etc., see Gaiser (1990), Horne et al. (1998). We are aware that the assumption of vertical inhomogeneity of the medium may represent a limiting condition of applicability of the proposed procedure. Generalization of the procedure to laterally varying and generally but weakly anisotropic structures is under preparation, see Pšenčík and Zheng (1999).

ACKNOWLEDGEMENTS

This work was supported by the consortium project "Seismic waves in complex 3-D structures (SW3D)". XZ is greateful for the support of the National Natural Science Foundation of China, No.49774230.

REFERENCES

Gaiser,J.E., 1990. Transversely isotropic phase velocity analysis from slowness estimates. *J. Geophys. Res.*, **95**, 11241-11254.

Gajewski,D. & Pšenčík,I., 1990. Vertical seismic profile synthetics by dynamic ray tracing in laterally varying layered anisotropic structures. *J.geophys.Res.*, **95**, 11301-11315.

Horne,S.A., McGarrity,J.P., Sayers,C.M., Smith,R.L. & Wijnands,F., 1998. Fractured reservoir characterisation using multi-azimuthal walkaway VSPs. 68th Ann. Internat. Mtg., Soc.Expl.Geophys., Expanded Abstracts, 1795-1798.

Liu,J. and Pšenčík,I., 1999. Inversion of qP wave travel times: synthetic study. In: Seismic Waves in Complex 3-D Structures, Report 8, pp.000-000, Dept.of Geophysics, Charles University Prague.

Pšenčík,I. & Gajewski,D., 1998. Polarization, phase velocity and NMO velocity of qP waves in arbitrary weakly anisotropic media. *Geophysics*, **63**, 1754-1766.

Pšenčík,I. & Zheng,X., 1998. Determination of weak anisotropy parameters from the qP wave particle motion measurements. In: Seismic Waves in Complex 3-D Structures, Report 7, pp.299-305, Dept.of Geophysics, Charles University Prague.

Pšenčík,I. & Zheng,X., 1999. Determination of weak anisotropy parameters from the qP wave slowness and particle motion measurements in laterally inhomogeneous media. In: Seismic Waves in Complex 3-D Structures, Report 8, pp.63-68, Dept.of Geophysics, Charles University Prague.

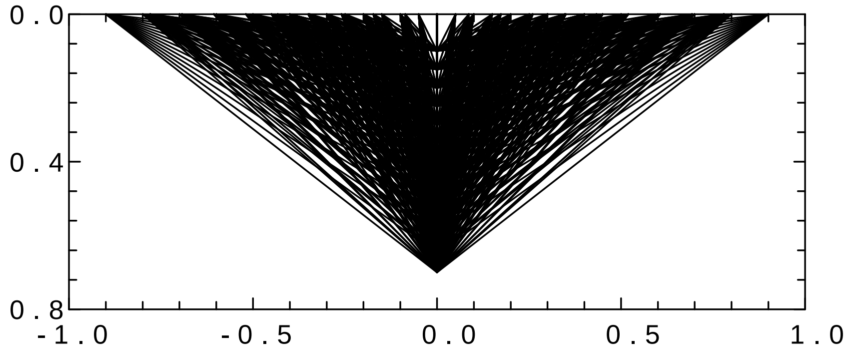

Straight-line connections
of source-receiver pairs in (x,z) plane

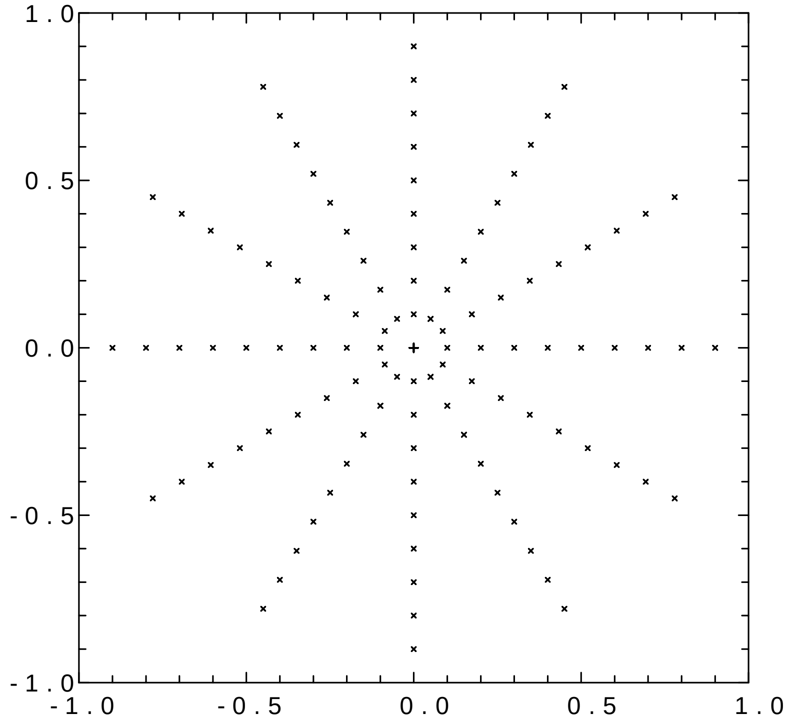

Position of sources and the borehole in (x,y) plane

Figure 1

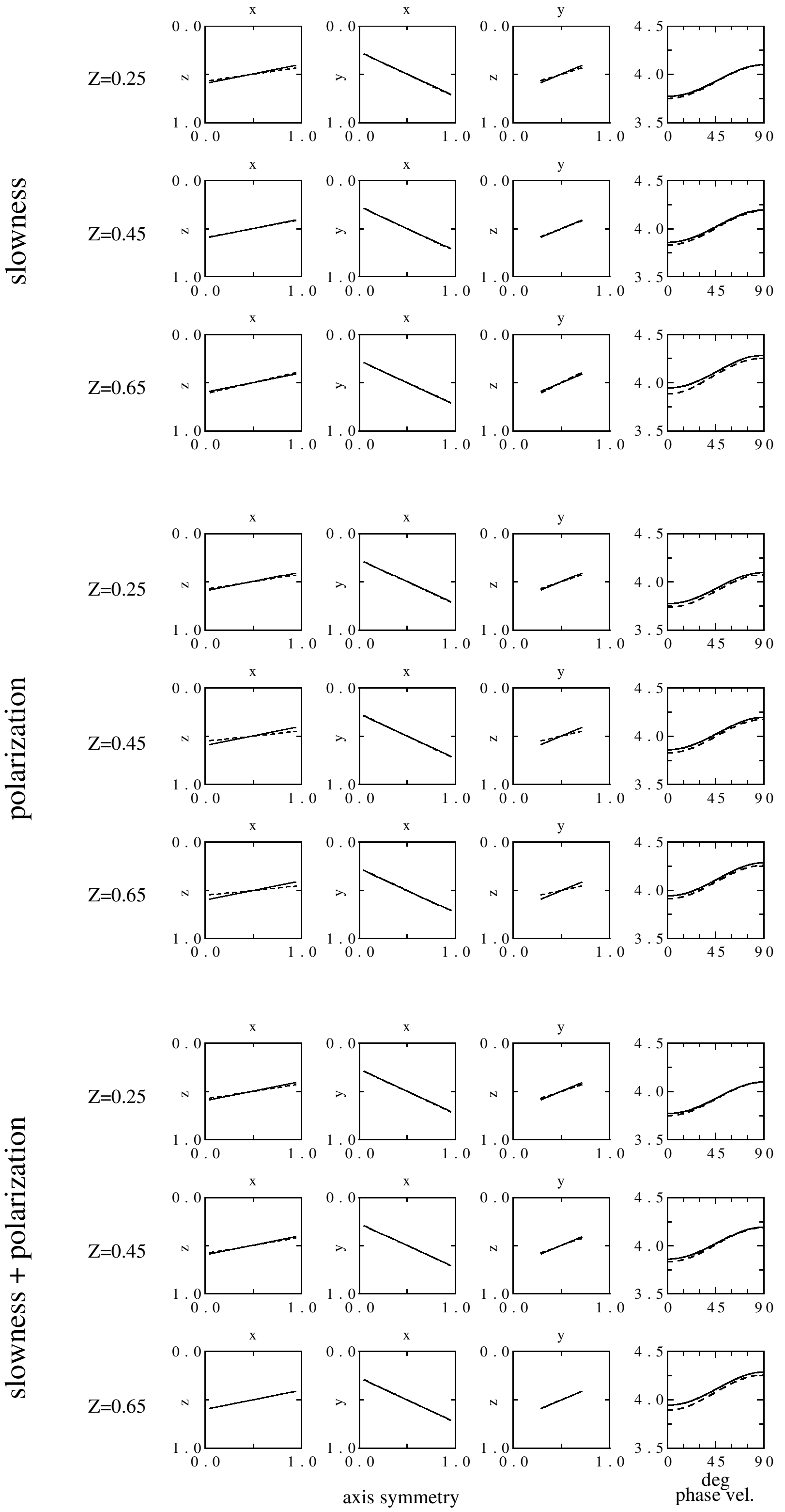

Figure 2. Comparison of exact (full lines) and inverted (dashed lines) projections of axis of symmetry (first three frames from the left) and phase velocity sections within the symmetry plane (the frames on the right). The data from 6 profiles are used.

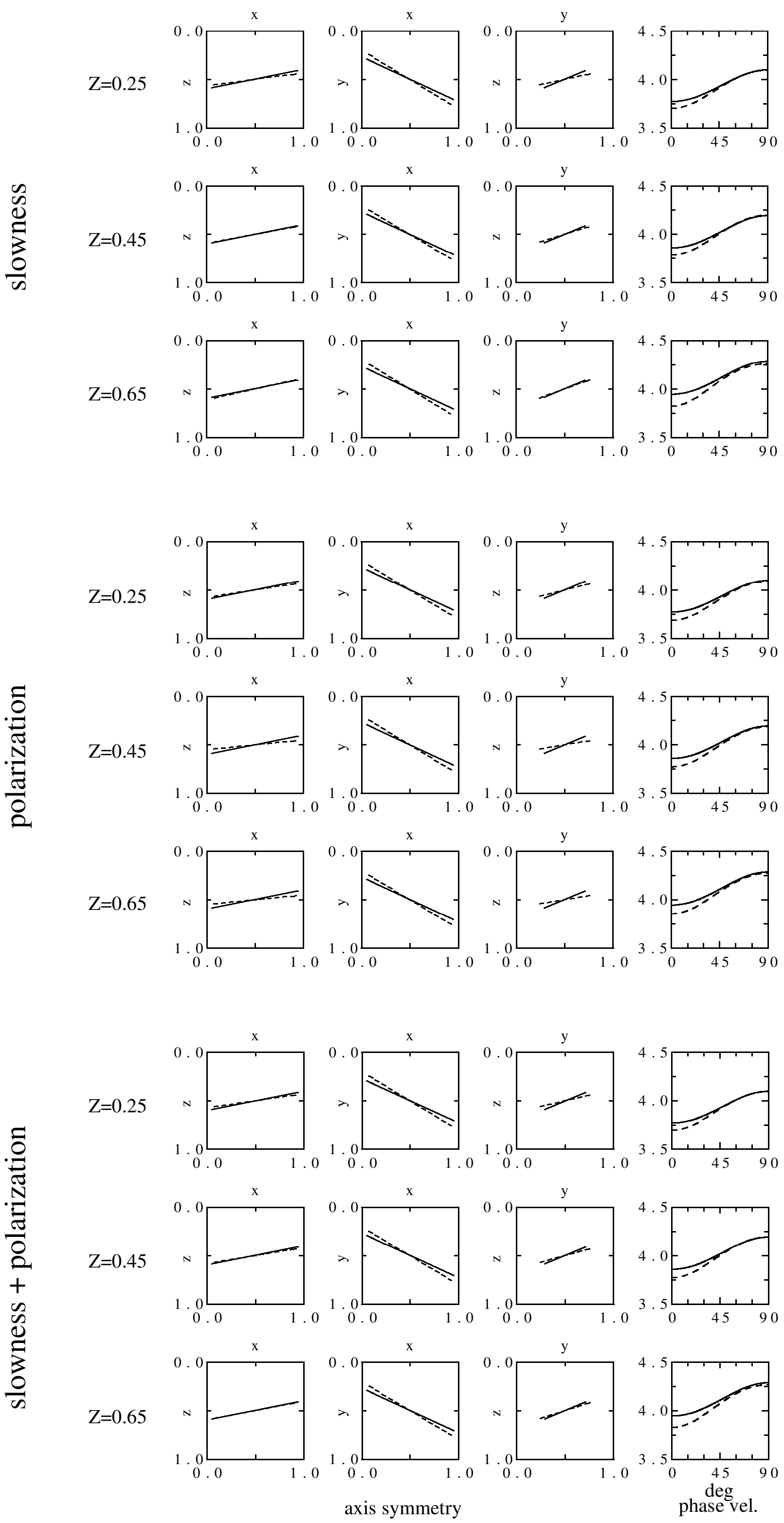

Figure 3. Comparison of exact (full lines) and inverted (dashed lines) projections of axis of symmetry (first three frames from the left) and phase velocity sections within the symmetry plane (the frames on the right). The data from 3 profiles are used.

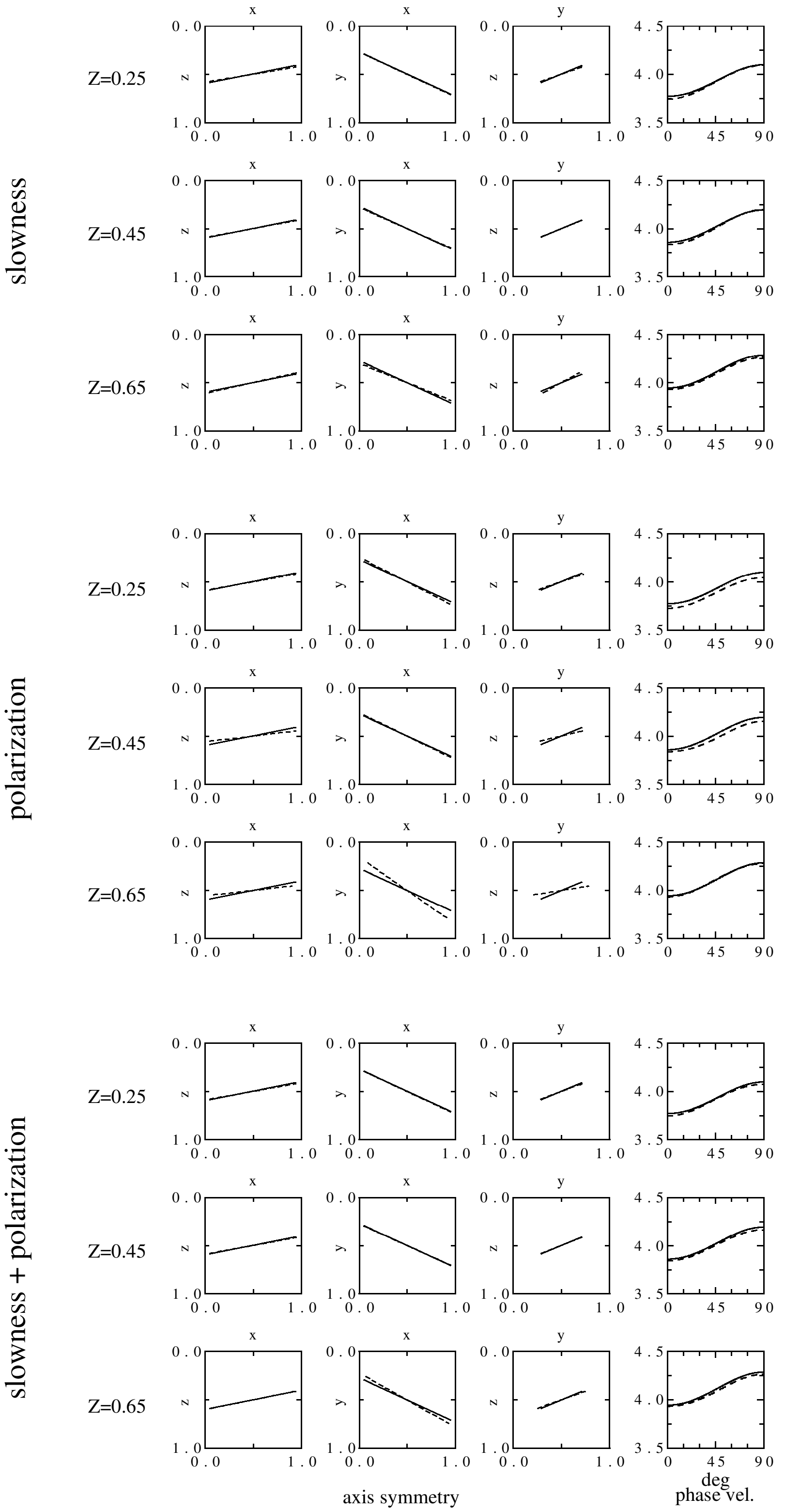

Figure 4. Comparison of exact (full lines) and inverted (dashed lines) projections of axis of symmetry (first three frames from the left) and phase velocity sections within the symmetry plane (the frames on the right). The data from 6 profiles and with 10% noise are used.

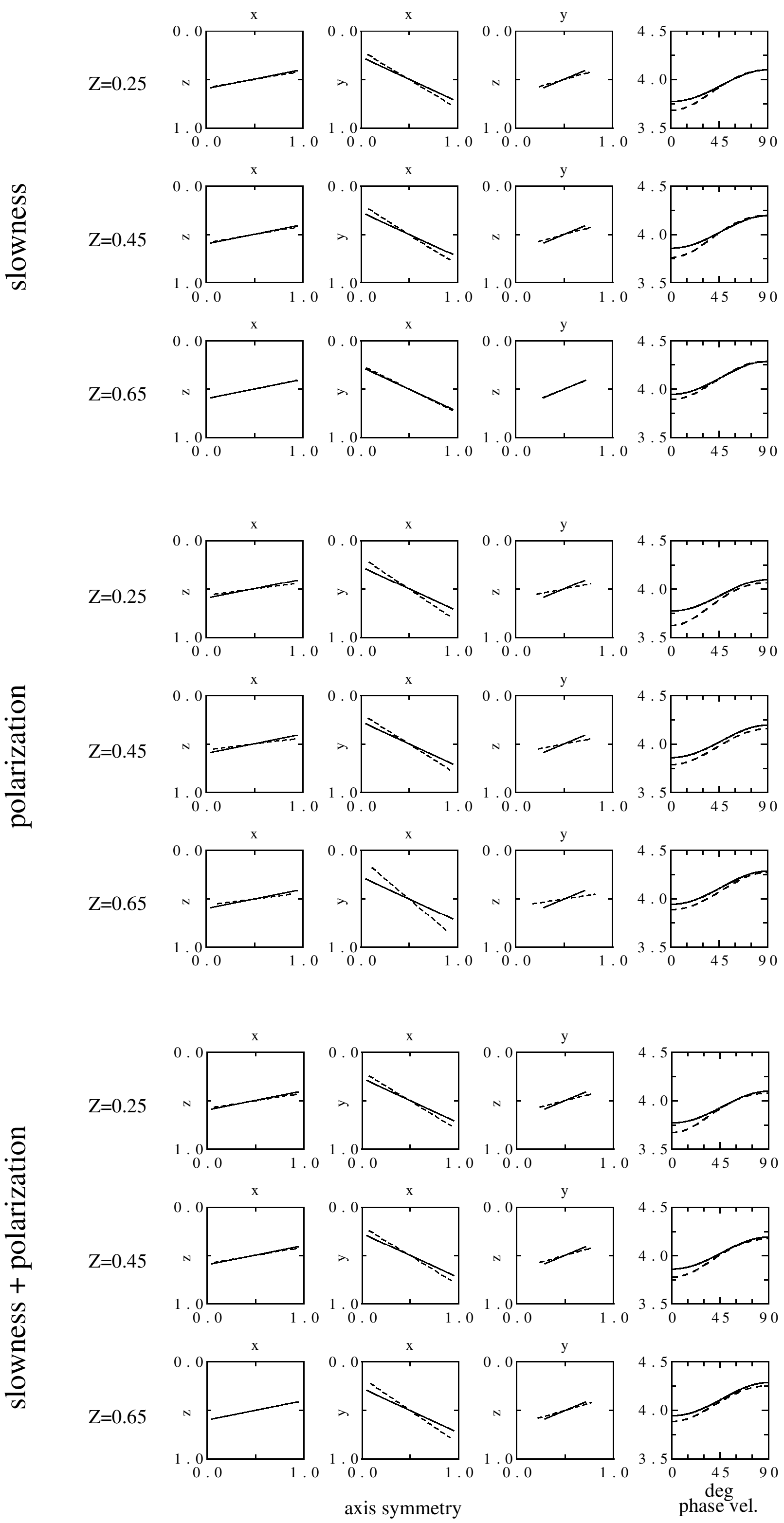

Figure 5. Comparison of exact (full lines) and inverted (dashed lines) projections of axis of symmetry (first three frames from the left) and phase velocity sections within the symmetry plane (the frames on the right). The data from 3 profiles and with 10% noise are used.

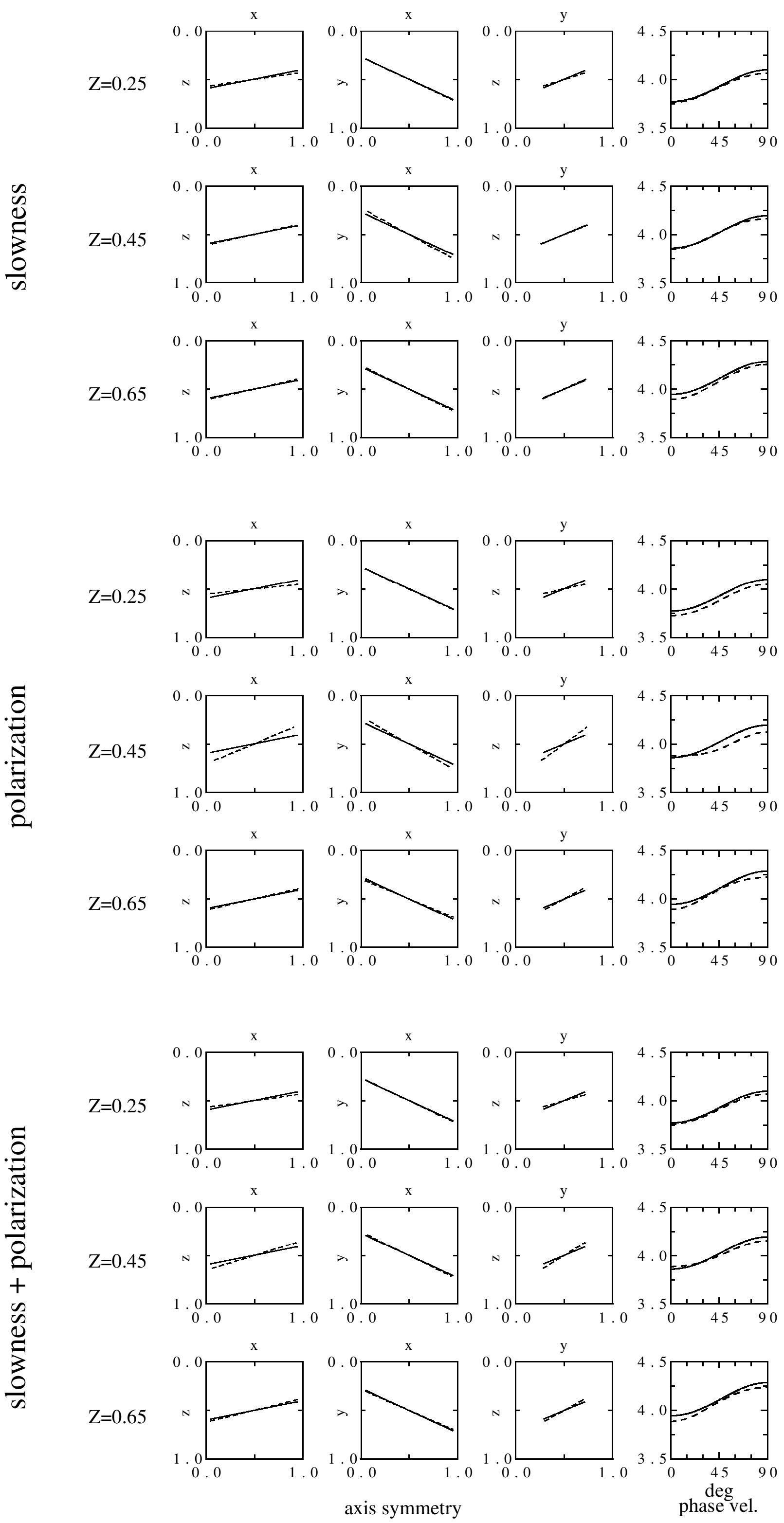

Figure 6. Comparison of exact (full lines) and inverted (dashed lines) projections of axis of symmetry (first three frames from the left) and phase velocity sections within the symmetry plane (the frames on the right). The data from 6 profiles and with 20% noise are used.

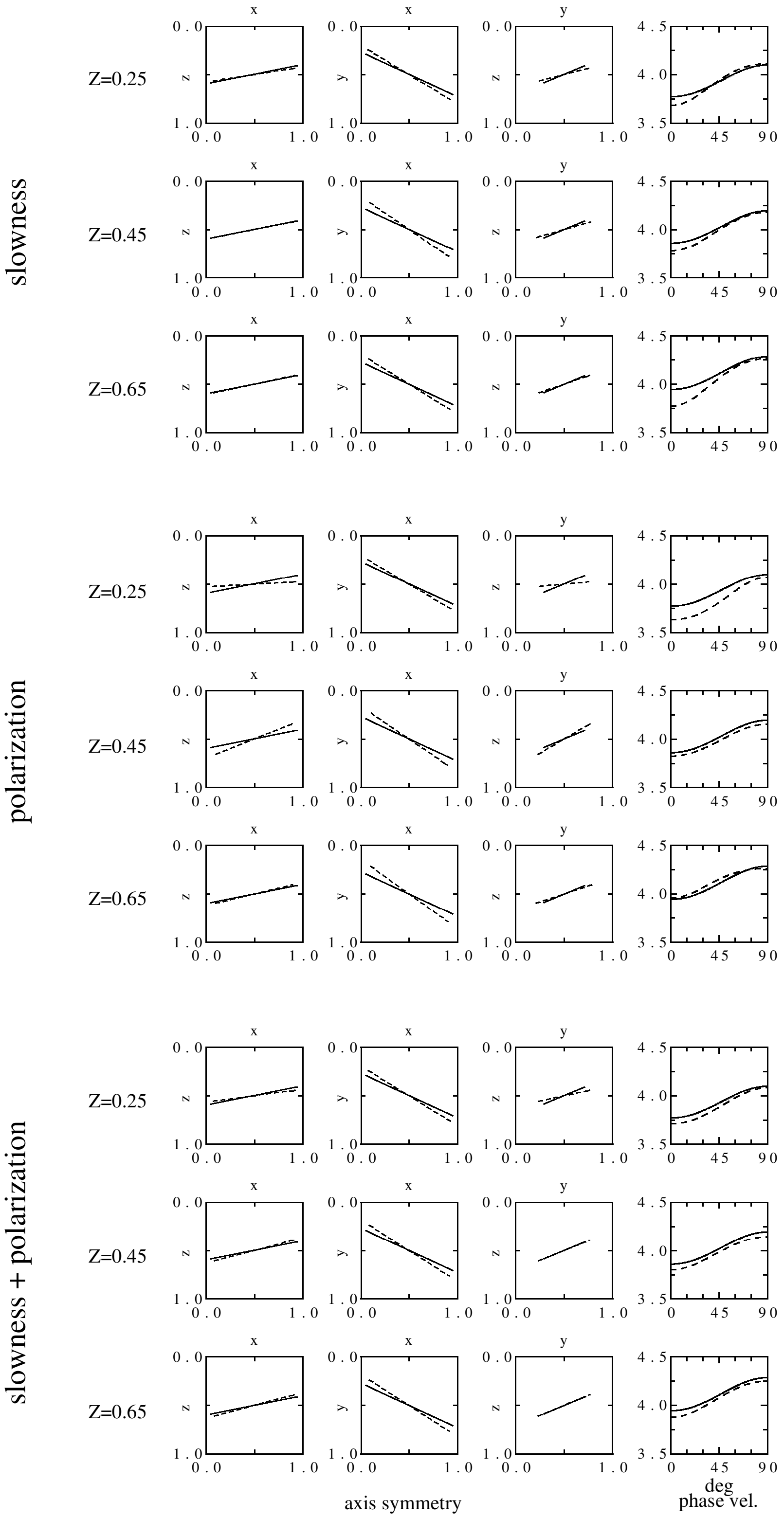

Figure 7. Comparison of exact (full lines) and inverted (dashed lines) projections of axis of symmetry (first three frames from the left) and phase velocity sections within the symmetry plane (the frames on the right). The data from 3 profiles and with 20% noise are used.

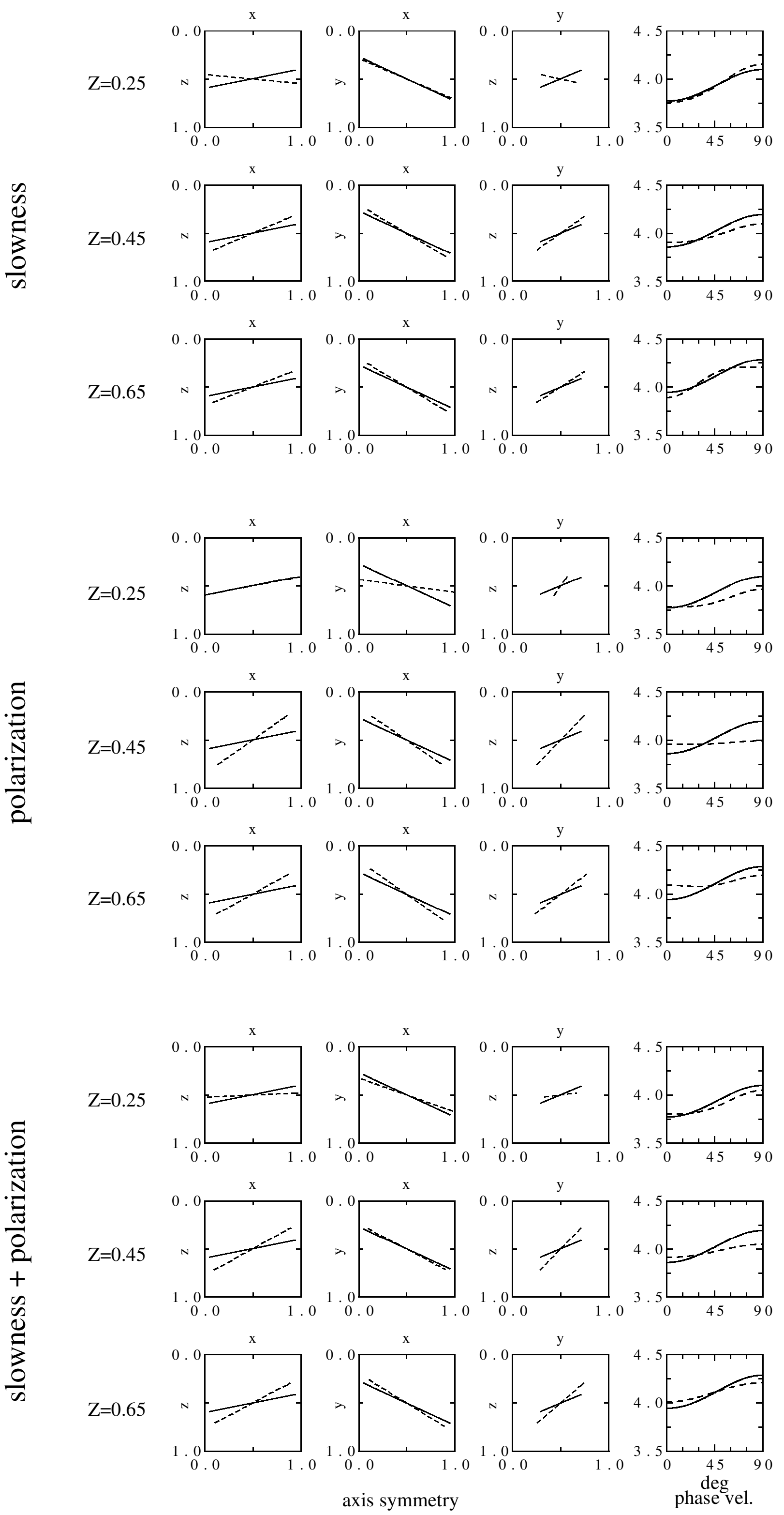

Figure 8. Comparison of exact (full lines) and inverted (dashed lines) projections of axis of symmetry (first three frames from the left) and phase velocity sections within the symmetry plane (the frames on the right). The data from 6 profiles and with 30% noise are used.

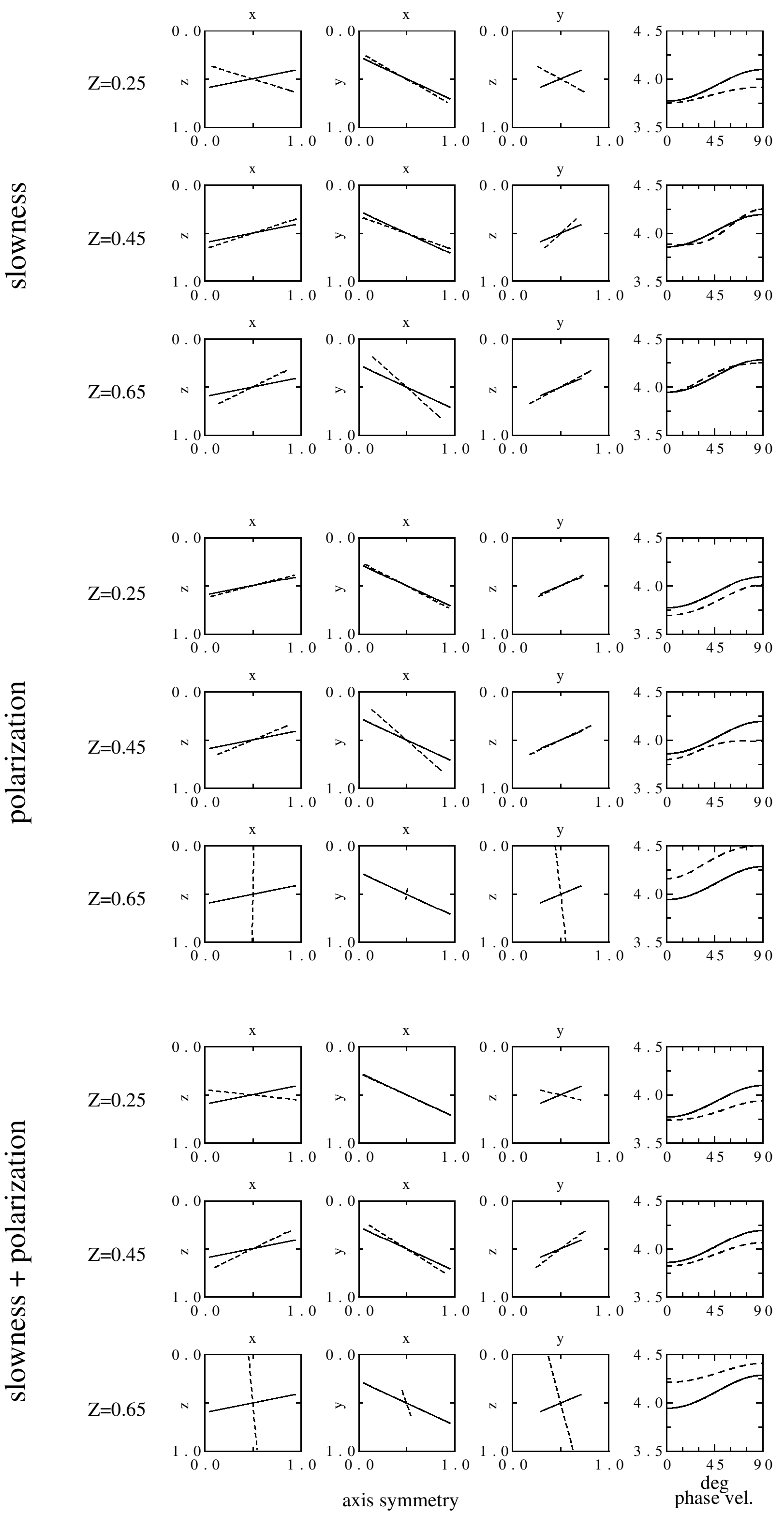

Figure 9. Comparison of exact (full lines) and inverted (dashed lines) projections of axis of symmetry (first three frames from the left) and phase velocity sections within the symmetry plane (the frames on the right). The data from 3 profiles and with 30% noise are used.